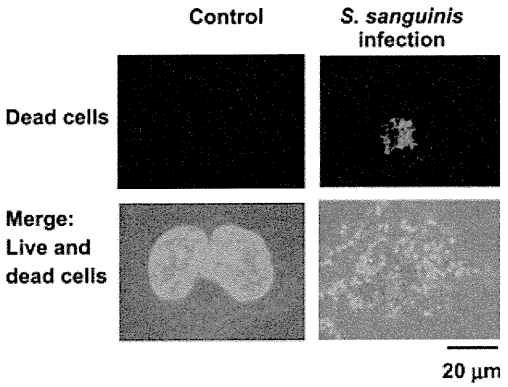

Fig. 3. Confocal micrographs of THP-1 macrophages infected with viable *Streptococcus sanguinis* SK36. THP-1 macrophages infected with *S. sanguinis* (MOI 200) and uninfected cells were first stained with PI, then treated with 0.1% Triton X100, and stained with DAPI. PI (magenta) stained the DNA of dead THP-1 cells, whereas DAPI (blue) stained that of both viable THP-1 and *S. sanguinis*.

cell death of macrophages (Ott *et al.*, 2007), we investigated the effect of an ROS inhibitor, DPI, on cell death. Infection with *S. sanguinis* in the presence of DPI resulted in a significant reduction of macrophage cytotoxicity (Fig. 5a), suggesting that ROS are involved in this process.

Activation of caspase-1

Pathogenic streptococci are reported to induce macrophage cell death through activation of caspase-1 and inflammasomes (Harder *et al.*, 2009). Therefore, we examined the cleavage of caspase-1 using Western blotting under several experimental conditions. However, we could not obtain clear evidence showing the activation of caspase-1 in the infected macrophages (Fig. 5b). These results suggested that the cell death process may be independent of caspase-1 activation.

Discussion

We found that *S. sanguinis* stimulated foam cell formation of macrophages, suggesting that this oral streptococcus may also contribute to atherosclerosis. In fact, oral streptococcal species including *S. sanguinis* have been detected in clinical specimens of atheromatous plaque (Chiu, 1999; Nakano *et al.*, 2006; Koren *et al.*, 2011). Moreover, foam cell formation was accelerated by heat-inactivated *S. sanguinis* as well as viable bacteria (Fig. 1). Activation of macrophages by bacterial components such as LPS has been reported to be sufficient to induce foam cell formation (Funk *et al.*, 1993; Kakayoglu & Byrne, 1998). Based on recent understanding of atherosclerosis as an inflammatory disease (Erridge, 2008), our results suggest that both live and dead *S. sanguinis* may be potential atherogenic stimuli, as each were shown to be promoters of inflammatory foam cell formation. Although the periodontal pathogen *P. gingivalis* is known to induce foam cell formation (Giacona *et al.*, 2004; Qi *et al.*, 2003), our literature search indicated that the involvement of oral streptococci in foam cell formation has not been reported. Thus, the molecular mechanism by which *S. sanguinis* induces foam cell formation requires further investigation.

Our subsequent experiment revealed that infection with viable *S. sanguinis* at higher doses (MOI > 100) induced cell death of differentiated THP-1 macrophages (Fig. 2).

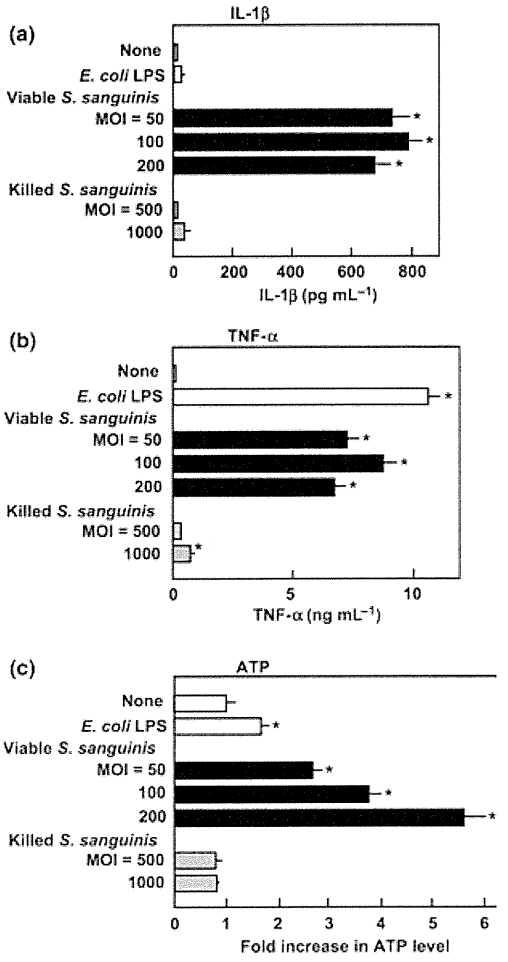

Fig. 4. Induction of IL-1β, TNF-α, and ATP by infection with *Streptococcus sanguinis*. Differentiated THP-1 macrophages were infected with viable *S. sanguinis* SK36 or stimulated with heat-inactivated *S. sanguinis* for 2 h, washed, and cultured for a further 18 h. The release of IL-1β (a) and TNF-α (b) was determined using an ELISA kit. ATP levels (c) in the culture supernatants were determined using an ATP measurement kit. Data are shown as the mean ± SD of triplicate samples. $*P < 0.05$ when compared with untreated control (none).

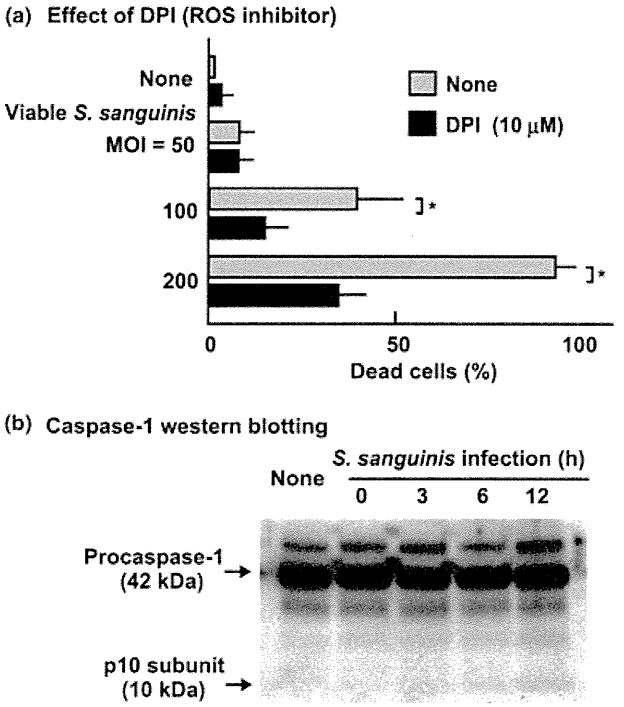

Fig. 5. Involvement of ROS production and caspase-1 activation in cell death induced by *Streptococcus sanguinis*. (a) Effect of ROS inhibitor. Differentiated THP-1 macrophages were infected with viable *S. sanguinis* SK36 for 2 h in the presence of DPI (10 μM), washed, and incubated for a further 18 h in the presence of antibiotics and DPI. Viability of the macrophages was determined using a trypan blue dye exclusion method. Data are shown as the mean ± SD of triplicate samples. $*P < 0.05$. (b) Western blot analysis of caspase-1. Macrophages were infected with *S. sanguinis* SK36 (MOI 100) for 2 h, washed, and incubated for a further 1 h (total 3 h), 4 h (total 6 h) or 10 h (total 12 h) in the presence of antibiotics. Lysates of macrophages were resolved using SDS-PAGE, transferred on to PVDF membranes, and reacted with the anti-p10 subunit of human caspase-1. Procaspase-1 and the p10 subunit of caspase-1 are indicated by arrows.

Induction of cell death of macrophages may contribute to atherosclerosis, because several investigations have suggested that dead macrophages are involved in the development of atherosclerosis plaque (Tabas, 2010). Therefore, *S. sanguinis* is potentially able to stimulate the progression of atherosclerosis by inducing cell death of macrophages, as well as by stimulating foam cell formation.

Recent investigations have reported that several pathogenic streptococci and staphylococci induce cell death of macrophages (Fettucciari *et al.*, 2000; Craven *et al.*, 2009; Harder *et al.*, 2009). Those studies suggested that bacterial pore-inducing toxins such as streptolysin O, β-hemolysin and α-hemolysin trigger the cell death of infected macrophages. As *S. sanguinis* has no pore-forming toxins, our finding that *S. sanguinis*-induced cell death of macrophages was unexpected. Therefore, we examined the possible involvement of the cell death pathway in phagocytic cells. The initial recognition of microorganisms is mediated by pattern recognition receptors such as toll-like receptors, which recognize bacterial components (Ishii *et al.*, 2008). Another class of pattern recognition receptors, intracellular nucleotide-binding oligomerization receptors (NLRs), have been identified (Ishii *et al.*, 2008). A group of NLRs participates in the formation of protein complexes called inflammasomes, which mediate the induction of caspase-1 activation in response to microbial stimulation (Yu & Finlay, 2008; Schroder & Tschopp, 2010). In the present study, we found that *S. sanguinis* infection induced the secretion of IL-1β and ATP (Fig. 4), which are known to be implicated in activation of inflammasomes (Petrilli *et al.*, 2007). Therefore, we examined the activation of caspase-1, but could not obtain clear evidence for its activation (Fig. 5). These results suggested that the cell death process may not be associated with activation of inflammasomes, but rather that IL-1β and ATP are released from damaged cells.

Alternatively, oxidative stress may contribute to the cell death, because ROS inhibitor reduced the cell death of macrophages (Fig. 5). ROS generated from damaged mitochondoria are known to induce cell death in various ways (Ott *et al.*, 2007). In this regard, several oral streptococcal species including *S. sanguinis* are known to produce hydrogen peroxide (Chen *et al.*, 2011). This bacterial product is a possible candidate for the virulence factor that mediates cellular damage in macrophages, because *Streptococcus gordonii*, another oral streptococcus, is reported to induce cell death of endothelial cells by peroxidogenesis (Stinson *et al.*, 2003). Our preliminary study suggested that the concentrations of hydrogen peroxide in the culture supernatants of *S. sanguinis* were <5 μM under the conditions of the infection assay, although its effect on macrophages was unknown. The involvement of hydrogen peroxide produced by *S. sanguinis* in the cell death of infected macrophages should be investigated further. To evaluate the molecular mechanisms underlying *S. sanguinis*-induced cell death, further study on the mitochondorial dysfunction induced by this microorganism will be required.

Acknowledgements

This work was supported in part by Grants-in-Aid for Scientific Research (A) (#19209063), (B) (#20390465, #20390531) and (C) (#20592398), and Grants-in-Aid for Young Scientists (B) (#21792069, #21791786) from the Japan Society for the Promotion of Science. We thank Dr M. Killian for providing *S. sanguinis* strain SK36.

References

Chen L, Ge X, Dou Y, Wang X, Patel JR & Xu P (2011) Identification of hydrogen peroxide production-related genes in *Streptococcus sanguinis* and their functional relationship with pyruvate oxidase. *Microbiology* **157**: 13–20.

Chiu B (1999) Multiple infections in carotide atherosclerotic plaques. *Am Heart J* **138**: S534–S536.

Craven RR, Gao X, Allen IC, Gris D, Wardenburg JB, McElvania-Tekippe E, Ting JP & Duncan JA (2009) *Staphylococcus aureus* α-hemolysin activates the NLRP3-inflammasome in human and mouse monocytic cells. *PLoS ONE* **4**: e7446.

Douglas CW, Heath J, Hampton KK & Preston FE (1993) Identity of viridans streptococci isolated from cases of infective endocarditis. *J Med Microbiol* **39**: 179–182.

Dyson C, Barnes RA & Harrison GAJ (1999) Infective endocarditis: an epidemiological review of 128 episodes. *J Infect* **38**: 87–93.

Erridge C (2008) The roles of pathogen-associated molecular patterns in atherosclerosis. *Trends Cardiovasc Med* **18**: 52–56.

Fettucciari K, Rosati E, Scaringi L, Cornacchione P, Migliorati G, Sabatini R, Fetriconi I, Rossi R & Marconi P (2000) Group B *streptococcus* induces apoptosis in macrophages. *J Immunol* **165**: 3923–3933.

Funk JL, Feingold KR, Moser AH & Grunfeld C (1993) Lipopolysaccharide stimulation of RAW264.7 macrophages induces lipid accumulation and foam cell formation. *Atherosclerosis* **98**: 67–82.

Giacona MB, Papapanou PN, Lamster IB, Rong LL, D'Agati VD, Schmidt AM & Lalla E (2004) *Porphyromonas gingivalis* induces its uptake by human macrophages and promotes foam cell formation *in vitro*. *FEMS Microbiol Lett* **241**: 95–101.

Gibson FC III, Yumoto H, Takahashi Y, Chou HH & Genco CA (2005) Innate immune signaling and *Porphyromonas gingivalis*-accelated atherosclerosis. *J Dent Res* **85**: 106–121.

Hajishengallis G, Sharma A, Russell MS & Genco RJ (2002) Interactions of oral pathogens with toll-like recepotors: possible role in atherosclerosis. *Ann Periodontol* **7**: 72–78.

Hancock JT & Jones OT (1987) The inhibition by diphenyleneiodonium and its analogues of superoxide generation by macrophages. *Biochem J* **242**: 103–107.

Harder J, Franchi L, Munoz-Planillo R, Park J-H, Reimer T & Nunez G (2009) Activation of the NLRP3 inflammasome by *Streptococcus pyogenes* required streptolysin O and NF-κB activation but proceeds independently of TLR signaling and P2X7 receptor. *J Immunol* **183**: 5823–5829.

Ishii KJ, Koyama S, Nakagawa A, Coban C & Akira S (2008) Host innate immune receptors and beyond: making sense of microbial infection. *Cell Host Microbe* **3**: 352–363.

Kakayoglu MV & Byrne GI (1998) A *Chlamydia pneumoniae* component that induces macrophage foam cell formation is chlamydial lipopolysaccharide. *Infect Immun* **66**: 5067–5072.

Kilian M, Mikkelsen L & Henrichsen J (1989) Taxonomic study of viridans streptococci; description of *Streptococcus gordonii* sp. nov. and emended descriptions of *Streptococcus sanguis* (White and Niven 1946), *Streptococcus oralis* (Bridge and Sneath 1982), and *Streptococcus mitis* (Andrewes and Horder 1906). *Int J Syst Bacteriol* **39**: 471–484.

Kolenbrander PE & London J (1993) Adhere today, here tomorrow: oral bacterial adherence. *J Bacteriol* **175**: 3247–3252.

Koren O, Spor A, Felin J *et al.* (2011) Microbes and health sackler colloquim: human oral, gut, and plaque microbiota in patients with atherosclerosis. *P Natl Acad Sci USA* **108**: 4592–4598.

Nakano K, Inaba H, Nomura R *et al.* (2006) Detection of cariogenic *Streptococcus mutans* in extirpated heart valve and atheromatous plaque specimens. *J Clin Microbiol* **44**: 3313–3317.

Nobbs AH, Lamont RJ & Jenkinson HF (2009) Streptococcus adherence and colonization. *Microbiol Mol Biol Rev* **73**: 407–450.

Okahashi N, Sakurai A, Nakagawa I, Fujiwara T, Kawabata S, Amano A & Hamada S (2003) Infection by *Streptococcus pyogenes* induces the receptor activator of NF-κB ligand expression in mouse osteoblastic cells. *Infect Immun* **71**: 948–955.

Ott M, Gogvadze V, Orrenius S & Zhivotovsky B (2007) Mitochondoria, oxidative stress and cell death. *Apoptosis* **12**: 913–922.

Petrilli V, Dostert C, Muruve DA & Tschopp J (2007) The inflammasome: a danger sensing complex triggering innate immunity. *Curr Opin Immunol* **19**: 615–622.

Qi M, Miyakawa H & Kuramitsu HK (2003) *Porphyromonas gingivalis* induces murine macrophage foam cell formation. *Microb Pathog* **35**: 259–267.

Schroder K & Tschopp J (2010) The inflammasome. *Cell* **140**: 821–832.

Stinson MW, Alder S & Kumar S (2003) Invasion and killing of human endothelial cells by viridans group of streptococci. *Infect Immun* **71**: 2365–2372.

Tabas I (2010) Macrophage death and defective inflammation resolution in atherosclerosis. *Nat Rev Immunol* **10**: 36–45.

Yu HB & Finlay BB (2008) The caspase-1 inflammasome: a pilot of innate immune responses. *Cell Host Microbe* **4**: 198–208.

International Scholarly Research Network
ISRN Dentistry
Volume 2011, Article ID 870364, 6 pages
doi:10.5402/2011/870364

Research Article

Bactericidal Effects of Diode Laser Irradiation on *Enterococcus faecalis* Using Periapical Lesion Defect Model

Masato Nagayoshi,[1] Tatsuji Nishihara,[2] Keisuke Nakashima,[3] Shigetsugu Iwaki,[4] Ker-Kong Chen,[5] Masamichi Terashita,[6] and Chiaki Kitamura[1]

[1] *Division of Pulp Biology, Operative Dentistry, and Endodontics, Department of Cariology and Periodontology, Kyushu Dental College, 2-6-1 Manazuru, Kokurakita, Kitakyushu 803-8580, Japan*
[2] *Division of Infections and Molecular Biology, Department of Health Promotion, Kyushu Dental College, 2-6-1 Manazuru, Kokurakita, Kitakyushu 803-8580, Japan*
[3] *Division of Periodontology, Department of Cariology and Periodontology, Kyushu Dental College, 2-6-1 Manazuru, Kokurakita, Kitakyushu 803-8580, Japan*
[4] *Marketing Research Section, R&D Department, NISSIN DENTAL PRODUCTS INC., 22-1 miyabayashi, asahi, Kameoka, Kyoto 621-0001, Japan*
[5] *Department of Conservative Dentistry, Kaohsiung Medical University Hospital and College of Dental Medicine, Kaohsiung Medical University, Shih-Chuan 1st Road, Kaohsiung 80708, Taiwan*
[6] *Division of Comprehensive Dentistry, Department of Clinical Communication and Practice, Kyushu Dental College, 2-6-1 Manazuru, Kokurakita, Kitakyushu 803-8580, Japan*

Correspondence should be addressed to Chiaki Kitamura, chi-aki-k@kyu-dent.ac.jp

Received 13 May 2011; Accepted 19 June 2011

Academic Editor: A. Carrassi

Objective. Photodynamic therapy has been expanded for use in endodontic treatment. The aim of this study was to investigate the antimicrobial effects of diode laser irradiation on endodontic pathogens in periapical lesions using an *in vitro* apical lesion model. *Study Design. Enterococcus faecalis* in 0.5% semisolid agar with a photosensitizer was injected into apical lesion area of *in vitro* apical lesion model. The direct effects of irradiation with a diode laser as well as heat produced by irradiation on the viability of microorganisms in the lesions were analyzed. *Results.* The viability of *E. faecalis* was significantly reduced by the combination of a photosensitizer and laser irradiation. The temperature caused by irradiation rose, however, there were no cytotoxic effects of heat on the viability of *E. faecalis. Conclusion.* Our results suggest that utilization of a diode laser in combination with a photosensitizer may be useful for clinical treatment of periapical lesions.

1. Introduction

It is generally accepted that disinfecting processes are essential for successful root canal treatment, and antimicrobial irrigants to remove microorganisms are important for chemomechanical preparation of a root canal [1, 2]. Endodontic irrigants are required to have a broad spectrum of antimicrobial activities, as well as a relative lack of toxicity against sound periapical tissue. Sodium hypochlorite (NaOCl) is a major endodontic irrigant, however, it has cytotoxic and neurotoxic effects when extruded into periapical tissues [3, 4]. To develop a safe endodontic irrigants, ozonated water was previously examined as an endodontic irrigant and demonstrated to be a useful irrigant for removal of microorganisms from root canals without damage to other tissues [5]. However, it is also known that complete elimination of microorganisms from root canals and periapical lesions by antimicrobial irrigants only is difficult, because of the anatomical complexities of root canals, deep invasion of microorganisms into dentinal tubules, and formation of biofilms on the surface of root apex, resulting in persistent apical periodontitis [6–8]. In addition, several studies have reported that the lack of response of refractory periapical lesion is due to the in inaccessibility of the extraradicular microorganisms or to the presence of microorganisms [9–11].

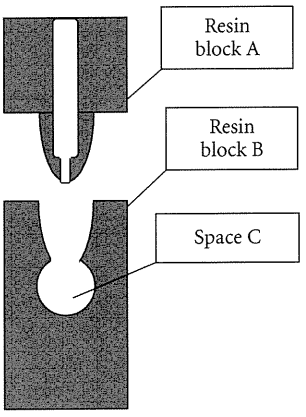

FIGURE 1: Schematic representation of present *in vitro* model of apical periodontitis. Resin block A, root part with a single root canal with an apical foramen (diameter 600 μm). Resin block B, periapical tissue portion with a space (Space C, diameter 5 mm) fashioned as a periapical lesion defect.

Recently, photodynamic antimicrobial chemotherapy has received focus as an alternate antibacterial, antifungal, and antiviral treatment for drug-resistant microorganisms [12, 13]. Along that line, disinfection of root canals by laser irradiation has been demonstrated [14–16]. When using laser irradiation for disinfection of root canals and periapical lesions, damage to periapical tissues by heat produced by the irradiation procedure should be avoided [17–19]. Several studies have reported the antimicrobial effectiveness and safety of laser irradiation of root canals. However, there are no known reports regarding the antimicrobial effects of laser irradiation on microorganisms in periapical lesions without corresponding heat damage to sound periapical tissues, because of difficulties in mimicking the related environment.

A few studies have reported that use of a photosensitizer in combination with laser irradiation was effective for selective elimination of microorganisms from root canals and periapical lesions [20–22]. The aim of this study was to investigate the antimicrobial effects of diode laser irradiation in combination with a photosensitizer against *Enterococcus faecalis*, one of the major organisms related to persistent apical periodontitis [10, 11, 23, 24] in periapical lesions using an *in vitro* apical lesion model. In addition, irradiation-induced heat changes and the effects of heat on *E. faecalis* were examined using our periapical lesion model.

2. Material and Methods

2.1. Light Source and Photosensitizer. The irradiation source was a diode laser (P-Laser; Panasonic Dental Co., Ltd., Osaka, Japan). Its wavelength, output power, and duty were 805 nm, 5 watts (W), and 20%, respectively, while the diameter of quartz optical fiber was 400 μm. Indocyanine green (Opthagreen®; Santen Pharmaceutical Co., Ltd., Osaka, Japan) (12.5 mg/mL), a commonly used fluorescent fundus contrast medium, was used as the photosensitizer.

2.2. Antimicrobial Activity of Laser Irradiation. *E. faecalis* ATCC 29212 was cultured in brain-heart infusion (BHI) broth (Difco, Detroit, MI) at 37°C for 18 hours in an atmosphere of 5% CO_2. The organisms were harvested by centrifugation at 10,000 ×g for 5 minutes then suspended in saline and adjusted to 3×10^6 cells/mL using a spectrophotometer. Bacterial cell suspensions were mixed with sterilized saline or indocyanine green solution in sterilized test tubes for a final suspension of 1.5×10^6 cells/mL, then individually irradiated by the diode laser at a distance of 1 mm for 30, 60, or 120 seconds. Following irradiation, each suspension (20 μL including 3×10^2 cells) was cultured on a BHI agar plate. The inoculated plates were incubated at 37°C for 18 hours in an atmosphere of 5% CO_2 and colony-forming units (CFU) counted using the spread plate method.

2.3. Laser Irradiation Using In Vitro Model of Periapical Lesion Defect. An *in vitro* model of a periapical lesion defect was fashioned from resin blocks (Nissin Dental Products, Inc., Kyoto, Japan) (Figure 1). It was made up of a single root canal with an apical foramen (diameter; 600 μm) in resin block A, which formed the root part of the model, while resin block B, which was used as the periapical tissue portion, had a space (Space C, diameter; 5 mm) fashioned as a periapical lesion defect. The model was sterilized before each experiment. *E. faecalis* was diluted to 2×10^6 cells/mL with prewarmed (45°C) BHI broth containing 1% agar, then 20 μL of the bacterial cell suspension was mixed with 20 μL of distilled saline or indocyanine green solution in Space C (final concentration of *E. faecalis*, 1×10^6 cells/mL). Resin block A was then inserted into resin block B and kept at room temperature.

The optical fiber of the diode laser was inserted into the root canal to reach its apex then microorganisms in Space C were irradiated for 30, 60, or 120 seconds. In addition, the model was also irrigated with sterilized saline (4 mL) or 2.5% NaOCl (4 mL) for 120 seconds as negative and positive controls, respectively. After each treatment, *E. faecalis* in Space C were diluted 1/100 with sterilized saline and subjected to vortexing for 5 minutes, then 20 μL of each sample (2×10^2 cells) was cultured on a BHI agar plate. CFU were determined after incubation of the inoculated plates at 37°C for 18 hours in an atmosphere of 5% CO_2.

2.4. Exposure of Microorganisms to Heat. *E. faecalis* suspensions were mixed with a sterilized indocyanine green solution (final suspension 1.5×10^6 cells/mL) and incubated in a heat block (TERMO ALUMI BATH ALB-220: IWAKI GLASS Co., Ltd. Japan) at 65°C for 60 seconds, after which heat-treated *E. faecalis* (20 μL; 3×10^2 cells) were cultured on BHI agar plates. The inoculated plates were then incubated at 37°C for 18 hours in an atmosphere of 5% CO_2 in air and CFU determined.

2.5. Temperature Monitoring during Laser Irradiation. Temperatures in the periapical lesion (Space C) and surrounding areas of the *in vitro* model were monitored during laser irradiation using infrared thermography (TH9100 WV: NEC Avio Infrared Technologies Co., Ltd. Japan). Just after performing laser irradiation, the inner temperature of the periapical lesion area (Space C) was also measured

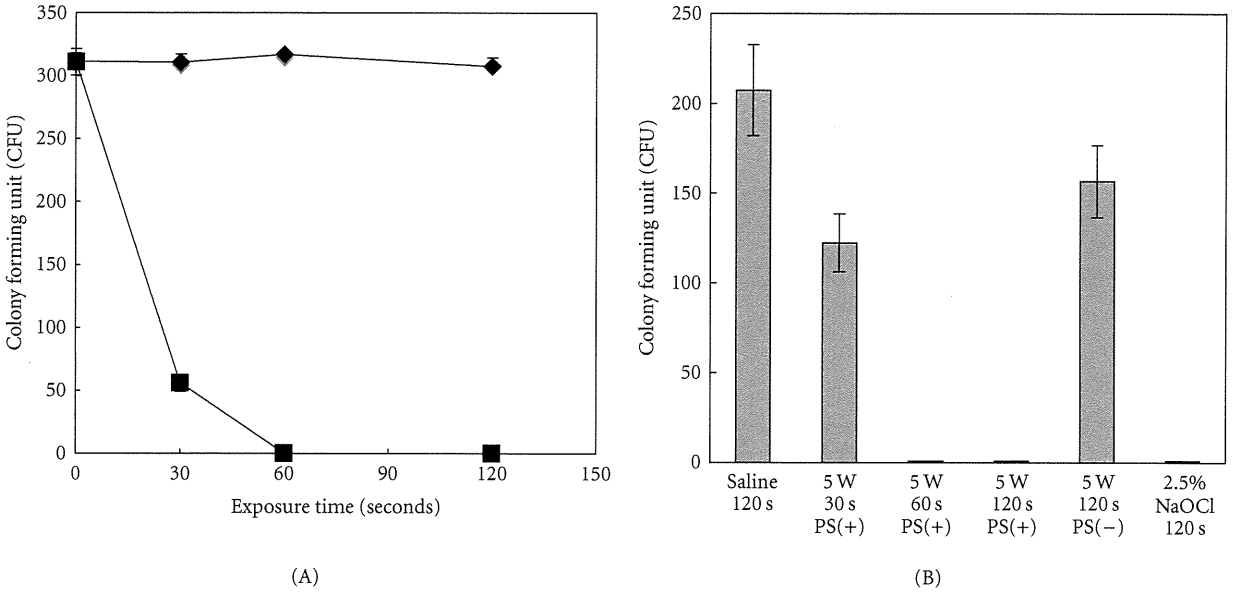

FIGURE 2: Antimicrobial effects of diode laser on *E. faecalis* in test tubes. The bacteria were exposed to laser irradiation with or without an added photosensitizer (closed diamond, without photosensitizer; closed square, with photosensitizer) for 30, 60, and 120 seconds. (A) Elimination of *E. faecalis* in model of apical periodontitis. *E. faecalis* in the presence and absence of a photosensitizer[PS(−), without photosensitizer; PS(+), with photosensitizer] in the lesion defect area of the model were exposed to diode laser irradiation for 30, 60, and 120 seconds. In addition, one sample was irrigated with sterilized saline for 120 seconds as a negative control (saline-120 s) and another with 2.5% NaOCl for 120 seconds as a positive control (2.5% NaOCl-120 s). (B) The number of viable cells after each treatment was counted. Data are expressed as the mean ± standard deviation of triplicate determinations. The experiment was performed three times, with similar results obtained in each.

by immediate insertion of a thermocouple thermometer (Digital Thermometer CT-800: As One Corp., Japan).

2.6. Statistical Analysis. Differences among variables in the experiments were compared using Student's *t*-test.

3. Results

3.1. Antimicrobial Effects of Diode Laser with Photosensitizer and Disinfection of Periapical Lesion Defect in In Vitro Model. There were no antimicrobial effects seen without the photosensitizer, whereas in its presence the cell viability of *E. faecalis* decreased to 72% after irradiation for 30 seconds and was not detected after irradiation of 60 seconds or more in test tubes (Figure 2(A)).

Figure 2(B) shows the antimicrobial effects of diode laser irradiation on *E. faecalis* in the *in vitro* model. Irrigation with saline did not have an antimicrobial effect, while that with NaOCl completely eliminated *E. faecalis*.When the diode laser was used without the photosensitizer for 120 seconds, the decrease in viability was only 25%. In contrast, a significant decrease in the viability of *E. faecalis* was observed following laser irradiation with the photosensitizer for 60 and 120 seconds.

3.2. Effects of Heat Produced by Laser Irradiation on Bacterial Cell Viability. The inner temperature of the apical lesion area of the *in vitro* model was determined with a thermocouple thermometer just after laser irradiation (Figure 3(A)). Irradiation for 60 seconds increased the temperature of the periapical lesion defect to 65°C. To analyze the cytotoxic effects of that elevated temperature (65°C) on *E. faecalis*, bacterial cells were incubated in a heat block at 65°C for 60 seconds (Figure 3(B)). There was no effect on bacterial cell viability by exposure to heating at 65°C, whereas the viability was significantly reduced when the bacterial cells were irradiated for 60 seconds in the presence of the photosensitizer. The rise in temperature in the periapical lesion and surrounding area of the *in vitro* model during laser irradiation was monitored using a thermotracer (Figure 3(C)). There was no change in temperature in either the lesion or surrounding area caused by irradiation when the photosensitizer was not added to the bacterial cell suspension (Figures 3(D)–3(F)). However, the thermotracer indicated an increase in temperature in the periapical lesion area with addition of the photosensitizer (Figures 3(G)–3(I)), which was 2°C after irradiation for 60 seconds and 6°C after that for 120 seconds (Figure 3(J)). In contrast, there was no rise in temperature observed in the area surrounding the lesion area even with addition of the photosensitizer (Figures 3(G)–3(I)).

4. Discussion

It is known that various photosensitizers are taken up by tumor cells and microorganisms, and those activated by laser irradiation interact with oxygen to produce radical species that have a toxic effect on those cells and microorganisms [25]. In the present study, indocyanine green, which was a photosensitizer commonly used as fluorescent fundus contrast medium that does not have toxicity toward surrounding tissues, increased the antimicrobial effects of laser irradiation

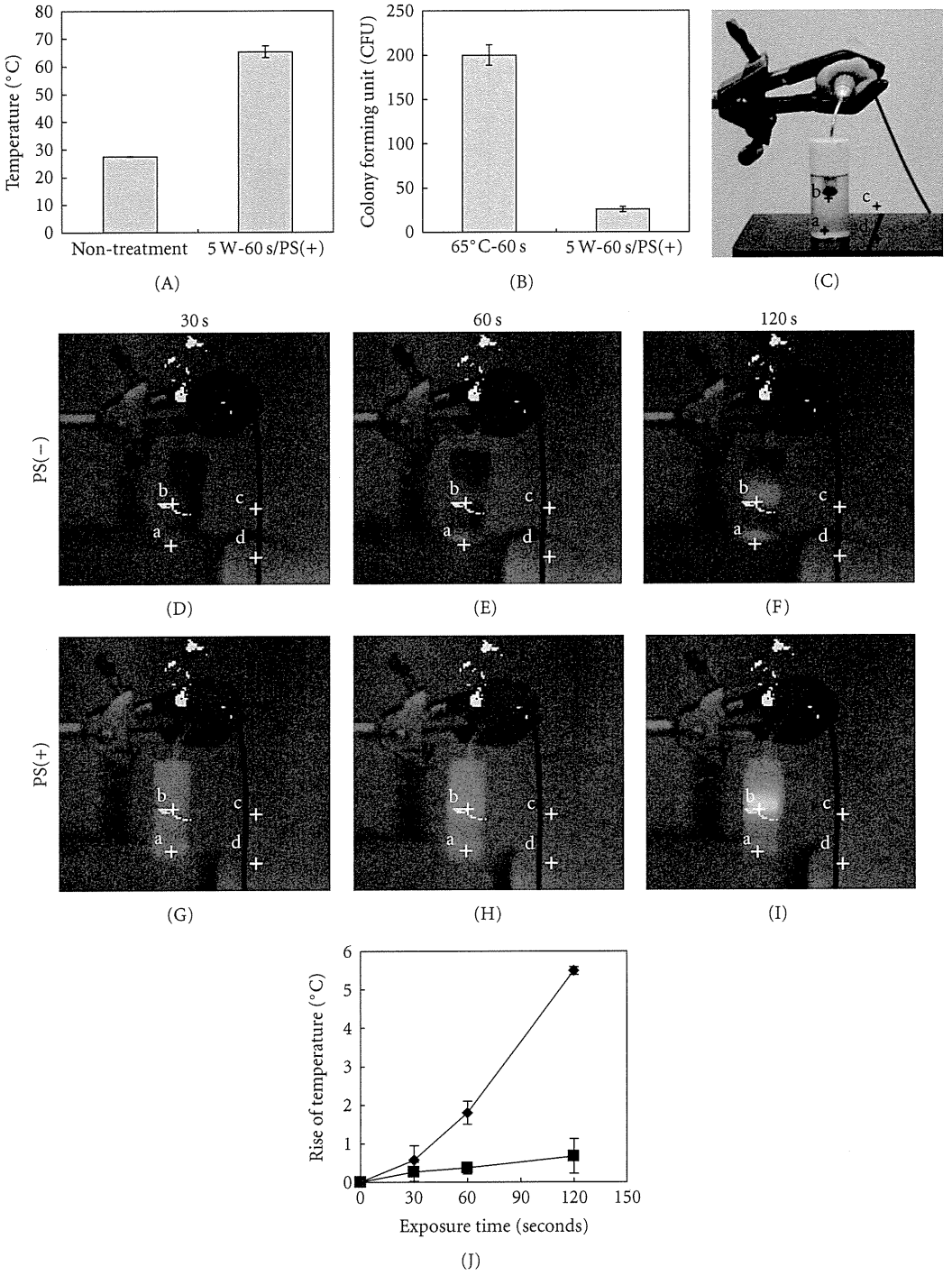

FIGURE 3: Effects of heat produced by laser irradiation. (A) Change of inner temperature in apical lesion area of *in vitro* model following laser irradiation. (B) Antimicrobial effects of heat on *E. faecalis*. The microorganisms were exposed to diode laser irradiation in the presence of a photosensitizer for 60 seconds [5 W-60 s/PS(+)] or exposed to heat at 65°C for 60 seconds (65°C-60 s). (C). Photograph of temperature change monitoring using a thermotracer, which was used to monitor 4 points (a, b, c, d) of the *in vitro* model. (D–F). Temperature change without photosensitizer. (G–I). Temperature change with photosensitizer. (J) Temperature change in periapical lesion area of the model during irradiation (closed diamond, with photosensitizer; closed square, without photosensitizer). The rise in temperature was calculated as the difference in temperature between points a and b. Data are expressed as the mean ± standard deviation of triplicate determinations. The experiment was performed three times, with similar results obtained in each.

in test tubes. However, that environment is different from that of a periapical lesion, which is surrounded by sound periapical tissues, and it takes many efforts to make a standardized apical lesion model *in vivo*.

To simulate biological conditions, we prepared an *in vitro* apical lesion model and examined the antimicrobial effects of diode laser irradiation with or without the addition of a photosensitizer. When a bacterial cell suspension with indocyanine green was irradiated with the diode laser using periapical lesion model, *E. faecalis* CFU were significantly decreased to the same amount following irrigation with NaOCl. In a study of bactericidal activity against *E. faecalis* biofilm in extracted human teeth, it was reported that the total energy output of a diode laser was 36J [26]. In the present study, an irradiation time of 60 seconds was employed to achieve a total energy level of 76J and that with an added photosensitizer was adequate for a high level of sterilization. On the other hand, application of the present diode laser for 60 seconds increased the temperature of the lesion area to 65°C. However, exposure of *E. faecalis* to 65°C for 60 seconds in a heat block did not have any effects on bacterial viability. These results indicate that the reduction in viability of *E. faecalis* was from the laser irradiation itself, not from the heat produced by the irradiation, and that addition of a photosensitizer is essential for the observed antimicrobial effects.

Adverse effects of intense heat produced by laser irradiation on sound periapical tissues are a concern in clinical applications. It has been reported that use of a diode laser resulted in the least amount of temperature increase among several types of lasers tested [19]. In the present study, it was found that irradiation at 5 W for 60 seconds in the presence of a photosensitizer raised it by 2°C in the lesion defect area, whereas no change in temperature was observed in the surrounding area. Furthermore, it has been demonstrated that the same diode laser irradiation with various levels of laser power (0.5 W to 5 W) for 2 minutes did not affect proliferation of mammalian cells *in vitro* and enhanced BMP-induced osteoblast differentiation by stimulating BMP/Smad signaling pathway [27]. Taken together, the present laser technique, which was adequate for elimination of *E. faecalis*, may have no cytotoxic effects on sound periapical tissues.

In conclusion, diode laser irradiation in combination with a photosensitizer had nearly the same antimicrobial effect as 2.5% NaOCl. Many clinicians prefer a diluted concentration to reduce the irritation potential of NaOCl, with 2.5% commonly recommended [28]. However, fibroblasts were found damaged by 2.5% NaOCl [3, 5, 28–30]. The present results indicated no cytotoxic effects from heat produced by laser irradiation, thus use of a diode laser with a photosensitizer is useful for treatment of periapical lesions without adverse effects on surrounding tissues. This standardized *in vitro* apical lesion model needs more improvement, but it may be useful for an endodontic study.

Acknowledgments

This investigation was supported in part by a Grant-in-Aid for Scientific Research (21592428) from The Ministry of Education, Culture, Sports, Science and Technology of Japan.

References

[1] T. W. Chow, "Mechanical effectiveness of root canal irrigation," *Journal of Endodontics*, vol. 9, no. 11, pp. 475–479, 1983.

[2] J. F. Siqueira Jr., I. N. Rôças, S. R. Santos, K. C. Lima, F. A. Magalhães, and M. de Uzeda, "Efficacy of instrumentation techniques and irrigation regimens in reducing the bacterial population within root canals," *Journal of Endodontics*, vol. 28, no. 3, pp. 181–184, 2002.

[3] A. Gatot, J. Arbelle, A. Leiberman, and I. Yanai-Inbar, "Effects of sodium hypochlorite on soft tissues after its inadvertent injection beyond the root apex," *Journal of Endodontics*, vol. 17, no. 11, pp. 573–574, 1991.

[4] E. J. Neaverth and R. Swindle, "A serious complication following the inadvertent injection of sodium hypochlorite outside the root canal system," *Compendium*, vol. 11, no. 8, pp. 474–481, 1990.

[5] M. Nagayoshi, C. Kitamura, T. Fukuizumi, T. Nishihara, and M. Terashita, "Antimicrobial effect of ozonated water on bacteria invading dentinal tubules," *Journal of Endodontics*, vol. 30, no. 11, pp. 778–781, 2004.

[6] N. Noguchi, Y. Noiri, M. Narimatsu, and S. Ebisu, "Identification and localization of extraradicular biofilm-forming bacteria associated with refractory endodontic pathogens," *Applied and Environmental Microbiology*, vol. 71, no. 12, pp. 8738–8743, 2005.

[7] Y. Noiri, A. Ehara, T. Kawahara, N. Takemura, and S. Ebisu, "Participation of bacterial biofilms in refractory and chronic periapical periodontitis," *Journal of Endodontics*, vol. 28, no. 10, pp. 679–683, 2002.

[8] F. J. Vertucci, "Root canal anatomy of the human permanent teeth," *Oral Surgery Oral Medicine and Oral Pathology*, vol. 58, no. 5, pp. 589–599, 1984.

[9] R. Fujii, Y. Saito, Y. Tokura, K. I. Nakagawa, K. Okuda, and K. Ishihara, "Characterization of bacterial flora in persistent apical periodontitis lesions," *Oral Microbiology and Immunology*, vol. 24, no. 6, pp. 502–505, 2009.

[10] K. Subramanian and A. K. Mickel, "Molecular analysis of persistent periradicular lesions and root ends reveals a diverse microbial profile," *Journal of Endodontics*, vol. 35, no. 7, pp. 950–957, 2009.

[11] P. T. Sunde, I. Olsen, G. J. Debelian, and L. Tronstad, "Microbiota of periapical lesions refractory to endodontic therapy," *Journal of Endodontics*, vol. 28, no. 4, pp. 304–310, 2002.

[12] M. Wainwright, "Photodynamic antimicrobial chemotherapy (PACT)," *Journal of Antimicrobial Chemotherapy*, vol. 42, no. 1, pp. 13–28, 1998.

[13] M. Wainwright and K. B. Crossley, "Photosensitising agents—circumventing resistance and breaking down biofilms: a review," *International Biodeterioration and Biodegradation*, vol. 53, no. 2, pp. 119–126, 2004.

[14] E. B. de Souza, S. Cai, M. R.L. Simionato, and J. L. Lage-Marques, "High-power diode laser in the disinfection in depth of the root canal dentin," *Oral Surgery, Oral Medicine, Oral Pathology, Oral Radiology and Endodontology*, vol. 106, no. 1, pp. e68–e72, 2008.

[15] J. A. Williams, G. J. Pearson, and M. John Colles, "Antibacterial action of photoactivated disinfection {PAD} used on endodontic bacteria in planktonic suspension and in artificial

and human root canals," *Journal of Dentistry*, vol. 34, no. 6, pp. 363–371, 2006.

[16] L. Zhu, M. Tolba, D. Arola, M. Salloum, and F. Meza, "Evaluation of effectiveness of Er,Cr:YSGG laser for root canal disinfection: theoretical simulation of temperature elevations in root dentin," *Journal of Biomechanical Engineering*, vol. 131, no. 7, Article ID 710041, 2009.

[17] M. Kreisler, W. Kohnen, M. Beck et al., "Efficacy of $NaOCl/H_2O_2$ irrigation and GaAlAs laser in decontamination of root canals *in vitro*," *Lasers in Surgery and Medicine*, vol. 32, no. 3, pp. 189–196, 2003.

[18] U. Schoop, W. Kluger, S. Dervisbegovic et al., "Innovative wavelengths in endodontic treatment," *Lasers in Surgery and Medicine*, vol. 38, no. 6, pp. 624–630, 2006.

[19] U. Schoop, W. Kluger, A. Moritz, N. Nedjelik, A. Georgopoulos, and W. Sperr, "Bactericidal effect of different laser systems in the deep layers of dentin," *Lasers in Surgery and Medicine*, vol. 35, no. 2, pp. 111–116, 2004.

[20] J. L. Fimple, C. R. Fontana, F. Foschi et al., "Photodynamic treatment of endodontic polymicrobial infection *in vitro*," *Journal of Endodontics*, vol. 34, no. 6, pp. 728–734, 2008.

[21] A. Silva Garcez, S. C. Núñez, J. L. Lage-Marques, A. O. C. Jorge, and M. S. Ribeiro, "Efficiency of NaOCl and laser-assisted photosensitization on the reduction of Enterococcus faecalis *in vitro*," *Oral Surgery, Oral Medicine, Oral Pathology, Oral Radiology and Endodontology*, vol. 102, no. 4, pp. e93–e98, 2006.

[22] N. S. Soukos, P. S. Y. Chen, J. T. Morris et al., "Photodynamic therapy for endodontic disinfection," *Journal of Endodontics*, vol. 32, no. 10, pp. 979–984, 2006.

[23] R. M. Love, "Enterococcus faecalis—a mechanism for its role in endodontic failure," *International Endodontic Journal*, vol. 34, no. 5, pp. 399–405, 2001.

[24] I. N. Rôças, J. F. Siqueira Jr., and K. R. N. Santos, "Association of *Enterococcus faecalis* with different forms of periradicular diseases," *Journal of Endodontics*, vol. 30, no. 5, pp. 315–320, 2004.

[25] K. Konopka and T. Goslinski, "Photodynamic therapy in dentistry," *Journal of Dental Research*, vol. 86, no. 8, pp. 694–707, 2007.

[26] Z. Lim, J. L. Cheng, T. W. Lim et al., "Light activated disinfection: an alternative endodontic disinfection strategy," *Australian Dental Journal*, vol. 54, no. 2, pp. 108–114, 2009.

[27] S. Hirata, C. Kitamura, H. Fukushima et al., "Low-level laser irradiation enhances BMP-induced osteoblast differentiation by stimulating the BMP/Smad signaling pathway," *Journal of Cellular Biochemistry*, vol. 111, no. 6, pp. 1445–1452, 2010.

[28] G. L. Becker, S. Cohen, and R. Borer, "The sequelae of accidentally injecting sodium hypochlorite beyond the root apex: report of a case," *Oral Surgery Oral Medicine and Oral Pathology*, vol. 38, no. 4, pp. 633–638, 1974.

[29] R. E. Beltz, M. Torabinejad, and M. Pouresmail, "Quantitative analysis of the solubilizing action of MTAD, sodium hypochlorite, and EDTA on bovine pulp and dentin," *Journal of Endodontics*, vol. 29, no. 5, pp. 334–337, 2003.

[30] I. Heling, I. Rotstein, T. Dinur, Y. Szwec-Levine, and D. Steinberg, "Bactericidal and cytotoxic effects of sodium hypochlorite and sodium dichloroisocyanurate solutions *in vitro*," *Journal of Endodontics*, vol. 27, no. 4, pp. 278–280, 2001.

Apoptosis and survivability of human dental pulp cells under exposure to Bis-GMA

Junya YANO[1], Chiaki KITAMURA[1], Tatsuji NISHIHARA[2], Masayuki TOKUDA[3], Ayako WASHIO[1], Ker-Kong CHEN[4], Masamichi TERASHITA[5]

1- DDS, PhD, Division of Pulp Biology, Operative Dentistry, and Endodontics, Department of Cariology and Periodontology, Kyushu Dental College, Japan.
2- DDS, PhD, Division of Infections and Molecular Biology, Department of Health Promotion, Kyushu Dental College, Japan.
3- DDS, PhD, Department of Restorative Dentistry and Endodontology, Kagoshima University Graduate School of Medical and Dental Sciences, Japan.
4- DDS, PhD, Department of Conservative Dentistry, Kaohsiung Medical University Hospital and College of Dental Medicine, Kaohsiung Medical University, Kaohsiung, Taiwan.
5- DDS, PhD, Division of Comprehensive Dentistry, Department of Clinical Communication Practice, Kyushu Dental College, Japan.

Corresponding address: Chiaki Kitamura, DDS, PhD - Division of Pulp Biology, Operative Dentistry and Endodontics, Department of Cariology and Periodontology, Kyushu Dental College, 2-6-1 - Manazuru - Kokurakita - Kitakyushu - 803-8580 - Japan - Phone: 81-93-582-1131 - Fax: 81-93-581-5399 - e-mail: chi-aki-k@kyu-dent.ac.jp

Received: June 19, 2009 - Modification: March 19, 2010 - Accepted: March 27, 2010

ABSTRACT

Objective: In the present study, we examined whether 2, 2-bis [4-(2-hydroxy-3-methacryloxypropoxy) phenyl] propane (Bis-GMA) has effects on LSC2 cells, human dental pulp cell line. Material and Methods: The viability, cell cycle, and morphology of LSC2 cells were analyzed after exposure to several different concentrations of Bis-GMA. The recovery of viability of Bis-GMA exposed cells was also analyzed in the condition without Bis-GMA. Further, penetration of Bis-GMA to dentin disc was examined using isocratic high-performance liquid chromatography. Results: There was a concentration-dependent decrease in cell proliferation and an increase in cell number in the sub-G1 population after exposure to Bis-GMA. Furthermore, the cells showed typical characteristics of apoptotic cells after the exposure to high concentration of Bis-GMA. In contrast, cells exposed to lower concentrations of Bis-GMA recovered their viability after being cultured without Bis-GMA. We also found that Bis-GMA is capable of penetrating 1-mm-thick dentin discs, though the penetrated concentration was lower than that showing cytotoxicity. Conclusion: These results suggest that Bis-GMA has cytotoxic effects, though dental pulp exposed to lower concentrations is able to recover their viability when Bis-GMA is removed.

Key words: Apoptosis. Bis-GMA. Cell viability. Dental pulp.

INTRODUCTION

During restorative procedures for a carious tooth, dental pulp is exposed to a variety of stimulations such as heat stress produced by cavity preparation[2], and hypoxia produced by local anesthesia[1].

When composite resin is used as a restorative material, dentists sometimes note inflammatory responses of dental pulp, which are considered to be caused by microleakage at the interface between cavity walls and filled composite resin[8,10]. Other studies have suggested that unpolymerized resin monomers remaining on the cavity floor may irritate dental pulp cells directly or indirectly through dentin, resulting in inflammatory responses[9,12].

It has previously been reported that apoptosis of pulp cells was induced during pulp wound healing after cavity preparation[5], and that apoptosis of pulp cell line was induced by heat stress[6] and hypoxia[13]. It was also found that capping agents modified pulp apoptosis induction[7]. Apoptotic cells induced in dental pulp disappear during pulp wound healing processes, suggesting cytotoxic effects of external stimulations via residual dentin and the recovery of dental pulp viability. However, it is largely unknown whether dental pulp cells adversely affected by resin monomers can recover their viability. In the present study, we examined effects of resin monomer, 2, 2-bis [4-(2-hydroxy-3-methacryloxypropoxy) phenyl] propane (Bis-GMA), on the viability of human dental pulp cell line.

MATERIAL AND METHODS

Cell culture

LSC2 cells, a dental pulp cell line derived from human dental pulp[11], were maintained in Dulbecco's modified Eagle's medium (DMEM; Invitrogen Corp., Carlsbad, CA, USA) containing 10% heat-inactivated fetal calf serum (FCS), 100 µg/mL of streptomycin, and 100 U/mL of penicillin, and then incubated in a humidified atmosphere of 5% CO_2 at 37°C.

Cell proliferation assay

LSC2 cells ($2x10^4$ cells/well) were cultured in 96 well plate with a medium containing 5% FCS for 24 h, then the medium was exchanged to that containing 1% FCS. Several different concentrations (0.01, 0.02, 0.03, and 0.04 mmol/L) of Bis-GMA (Polyscience Inc., Warrington, PA, USA) diluted by dimethylsulfoxide (DMSO; Wako Pure Chemical Inc, Osaka, Japan) were added to the culture medium. At 48 h after exposure to Bis-GMA, cell proliferation was examined using the 5-bromo-2'-deoxyuridine (BrdU) assay (The Biotrak cell proliferation ELISA system version 2; GE Healthcare UK Ltd, UK). Cell viability was analyzed by measuring optical density (OD) using a test wavelength of 540 nm and a reference wavelength of 620 nm with a multiscan biochromatic microplate reader (Multiscan JX; Thermo Fisher Scientific K.K., Yokohama, Japan).

Cell cycle analysis

LSC2 cells were exposed to Bis-GMA for 48 h, then suspended in a hypotonic solution (0.1% Triton X-100, 1 mmol/L Tris/HCl, pH 8.0, 3.4 mmol/L sodium citrate, 0.1 mmol/L EDTA) and stained with 5 µg/mL of propidium iodide, after which cell-cycle distribution was analyzed with a FACScalibur flow cytometer EPICS XL (Beckman Coulter Inc., Brea, CA, USA).

Detection of cell death by hoechst staining

LSC2 cells were exposed to Bis-GMA in a chamber slides for 48 h, then fixed with 1% glutaraldehyde for 30 min, washed with 1x phosphate buffered saline (PBS), and stained with 5 g/mL of Hoechst dye 33342 (Life Technologies Co., CA, USA). Cells detached from the coverslips into the medium were also recovered by centrifugation and stained. Nuclei were observed under a fluorescence microscope (OLYMPUS BX50/BX-FLA/DP70; Olympus Co., Tokyo, Japan).

Cell recovery after removal of Bis-GMA from culture medium

After exposure of LSC2 cells to Bis-GMA for 48 h, the wells were rinsed by PBS, and added a medium containing 10% FCS without Bis-GMA. After the culture of surviving cells in a humidified atmosphere of 5% CO_2 at 37°C for 96 h, cell proliferation and cell cycle were analyzed.

Dentin penetration assay

Dentin discs (1 mm thick, minimum diameter: 6 mm) were cut from freshly extracted sound human third molars using a low speed diamond-coated saw (Isomet; Buehler, Lake Bluff, IL, USA) under water coolant, then etched for 60 s with 35% phosphoric acid to completely open dentinal tubules, rinsed with ultrasonication for 3 min in distilled water, and placed in the PFA tube (Sanplatec, Osaka, Japan). The lower chamber was filled with distilled water and the upper chamber with 0.2 mmol/L of Bis-GMA. After standing in a humid chamber at room temperature for 2 weeks, the distilled water was collected and mixed with chloroform to isolate Bis-GMA. Bis-GMA was detected using isocratic high-performance liquid chromatography (HPLC) (Waters, Milford, MA, USA) with a reverse-phase column (µ-Bondashere C18, 5 µm, 300 A column, JLC010032Y) (Waters) at 280 nm. The peak area

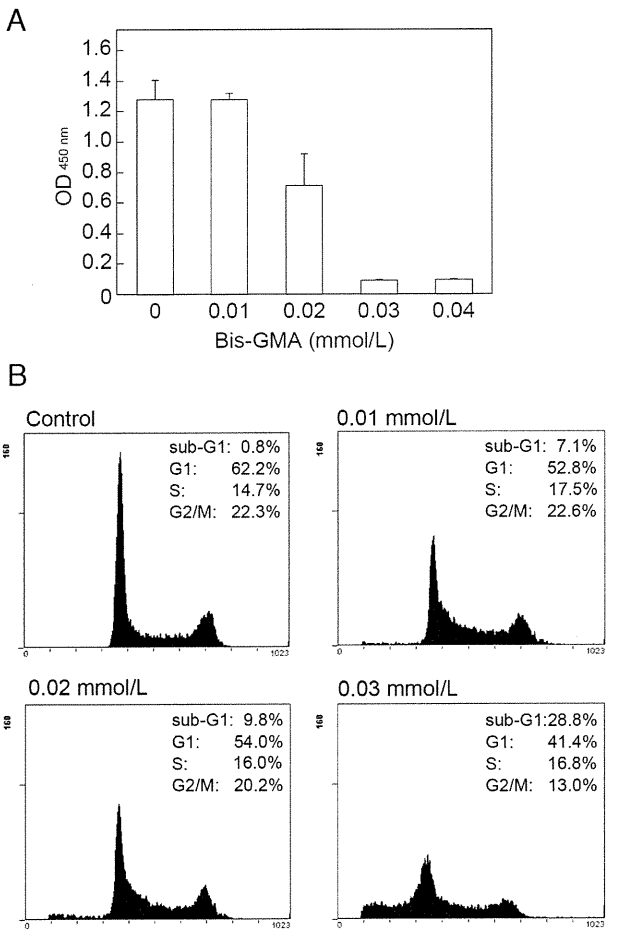

Figure 1- Cytotoxic effects of 2, 2-bis [4-(2-hydroxy-3-methacryloxypropoxy) phenyl] propane (Bis-GMA) on LSC2 cells. (A). Viability of LSC2 cells after exposure to Bis-GMA. (B). Cell cycle of LSC2 cells after exposure to Bis-GMA

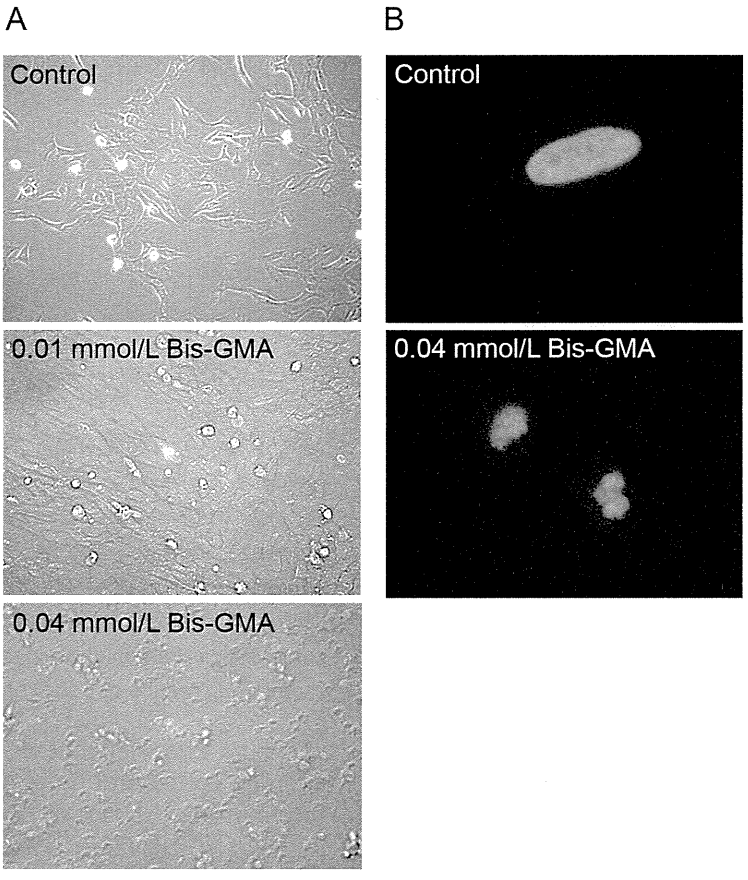

Figue 2- Morphological changes of LSC2 cells promoted by 2, 2-bis [4-(2-hydroxy-3-methacryloxypropoxy) phenyl] propane (Bis-GMA). (A). Phase-contrast microphotographs of LSC2 cells after exposure to Bis-GMA. Original magnification, x100. (B). Fluorescent microphotographs of LSC2 cells after exposure to Bis-GMA. Original magnification, x400

of Bis-GMA shown by HPLC tracing was analyzed using the Waters 2487 Dual λ absorbance detector (Waters), and the amount of Bis-GMA was calculated from the calibration curve of known concentrations from control experiments.

Statistical analysis

Statistical analysis of the data was performed using one-way ANOVA followed by a multiple-comparison Sheffe's test with Statview 5.0 software (SAS software Inc., Cary, NC, USA). Statistical significance was determined at $p<0.05$.

RESULTS

Cell death of human dental pulp cells after exposure to Bis-GMA

The viability of LSC2 cells decreased after exposure to Bis-GMA in a dose-dependent manner (Figure 1A). There was no significant difference ($p>0.05$) in viability between 0 and 0.01 mmol/L of Bis-GMA, whereas significant decreases of cell viability were observed after being cultured with 0.02, 0.03, and 0.04 mmol/L of Bis-GMA ($p<0.01$). The effects of exposure to Bis-GMA on cell cycle progression of LSC2 cells are shown in Figure 1B. Exposure to Bis-GMA reduced the number of the cells in G1, S, and G2/M phases in a dose-dependent manner, with a concomitant increase of those in the sub-G1 population, implying cell death such as apoptosis.

Morphological changes of LSC2 cells following exposure to Bis-GMA are shown in Figure 2. The structures of those cells exposed to 0.01 mmol/L of Bis-GMA were nearly the same as those of the control, whereas the rounding and the detachment were observed in cells exposed to 0.04 mmol/L of Bis-GMA (Figure 2A). Fluorescent microscopic analysis revealed that the nuclei of adhesive cells had normal structures, whereas those of cells that had fallen into the medium after exposure to 0.04 mmol/L of Bis-GMA showed fragmentation, a typical characteristic of apoptotic cells (Figure 2B).

Recovery of cell viability after the removal of Bis-GMA

Following exposure to Bis-GMA, surviving cells attached to the bottom of the well were cultured in normal condition without Bis-GMA (Figure 3A). The proliferation of surviving cells following exposure to 0.01 and 0.02 mmol/L of Bis-GMA was not different after 24 h of cell culture in normal condition, and

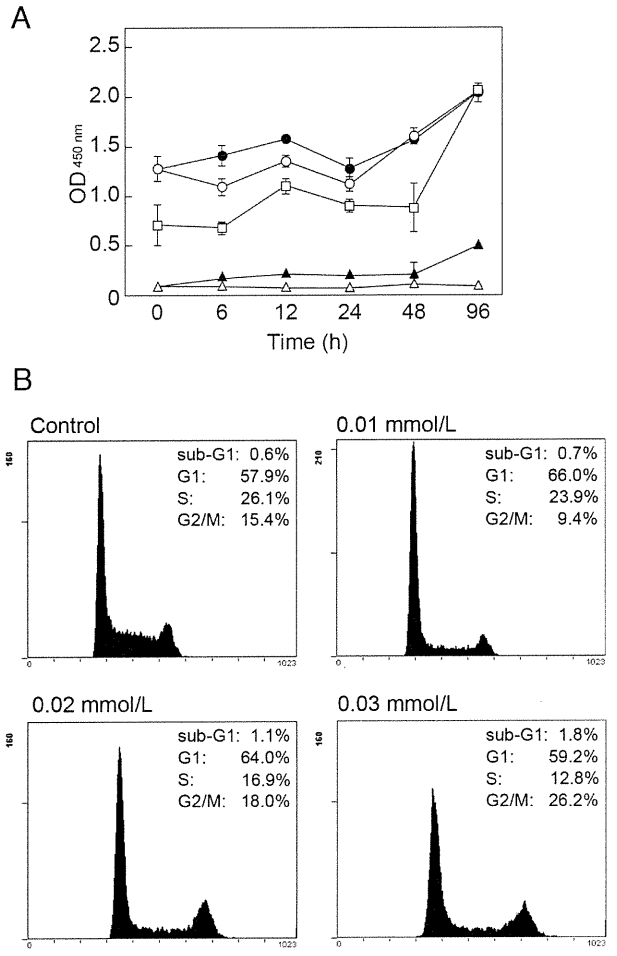

Figue 3- Survival of LSC2 cells against 2, 2-bis [4-(2-hydroxy-3-methacryloxypropoxy) phenyl] propane (Bis-GMA). (A). Recovery of viability of LSC2 cells that survived after exposure to Bis-GMA. Concentrations of Bis-GMA (mmol/L); 0 (black circle), 0.01 (white circle), 0.02 (white rectangle), 0.03 (black triangle), and 0.04 (white triangle). (B). Cell cycle of LSC2 cells that survived after exposure to Bis-GMA

then increased at 48 and 96 h, while surviving cells exposed to 0.03 mmol/L of Bis-GMA showed proliferation at 96 h. In contrast, exposure to 0.04 mmol/L of Bis-GMA showed great cytotoxicity on the viability of the cells, and proliferation was not recovered during the culture in the normal condition. The recovery of cell-cycle progression in surviving cells exposed to 0.01, 0.02, and 0.03 mmol/L of Bis-GMA was also observed (Figure 3B). When Bis-GMA-exposed cells were cultured in normal condition without Bis-GMA for 96 h, the cell cycle distribution pattern of Bis-GMA-insulted cells returned to that prior to exposure to Bis-GMA.

Dentin penetration of Bis-GMA through dentinal tubules

In the penetration model, Bis-GMA penetrated through 1 mm thick dentin disc. From the calibration

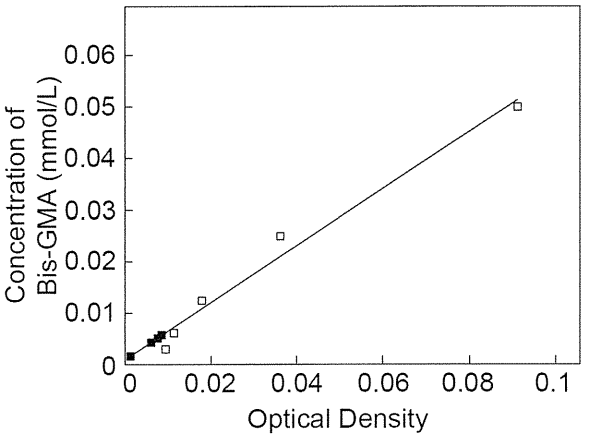

Figue 4- Calibration curve of known concentrations of 2, 2-bis [4-(2-hydroxy-3-methacryloxypropoxy) phenyl] propane (Bis-GMA) and concentrations of Bis-GMA that penetrated 1 mm dentin discs. White rectangles indicate known concentrations of control Bis-GMA for the calibration curve. Black rectangles indicate concentrations calculated from HPLC results of penetrated Bis-GMA

curve of known concentrations of Bis-GMA, the average concentration of penetrated Bis-GMA was 0.0043 mmol/L (Figure 4).

DISCUSSION

In the present study, it was found that exposure to high concentrations of Bis-GMA induced an increase in cell number in the sub-G1 population in cell-cycle, and the cell death with typical structures of apoptosis, suggesting that direct exposure to a high concentration of Bis-GMA induced apoptosis in human dental pulp cells.

It was also examined whether LSC2 cells exposed to Bis-GMA can recover their viability after the removal of Bis-GMA. We cultured surviving cells after exposure to Bis-GMA in the normal medium without Bis-GMA, and found that the cells exposed to 0.01, 0,02, and 0.03 mmol/L of Bis-GMA showed the recovery of the cell proliferation, whereas those exposed to 0.04 mmol/L of Bis-GMA did not recover their proliferation. In addition, cell-cycle of surviving cells after exposure to 0.01, 0.02, and 0.03 mmol/L of Bis-GMA returned to the same level as the control. These results suggest that even after the exposure to Bis-GMA, LSC2 cells have an ability to recover their viability when the concentration of Bis-GMA is low, whereas the cells exposed to high concentration of Bis-GMA lose such recovery ability.

Another finding of the present study was that the average concentration of Bis-GMA that penetrated 1 mm thick dentin was 0.0043 mmol/L, which was lower than the concentration used in the present study. These results are consistent with previous studies[3,4], and suggest that an adequate volume of

residual dentin thickness would be able to suppress the penetration of a harmful concentration of Bis-GMA.

Taken together, the findings of the present study suggest that dental pulp cells have the tolerance against lower concentrations of resin monomers, and that polymerized composite resin on the sufficient thickness of residual dentin may not be harmful to dental pulp.

CONCLUSION

These results produced evidence that Bis-GMA has cytotoxic effects, though dental pulp exposed to lower concentrations is able to recover their viability when Bis-GMA is removed.

ACKNOWLEDGEMENTS

This research was supported by Grants in Aid for Scientific Research 18209057 and 20592231 from The Ministry of Education, Science, and Culture of Japan, Tokyo, Japan.

REFERENCES

1- Agata H, Kagami H, Watanabe N, Ueda M. Effect of ischemic culture conditions on the survival and differentiation of porcine dental pulp-derived cells. Differentiation. 2008;76:981-93.

2- Amano T, Muramatsu T, Amemiya K, Kubo K, Shimono M. Responses of rat pulp cells to heat stress *in vitro*. J Dent Res. 2006;85:432-5.

3- Bouillaguet S, Wataha JC, Hanks CT, Ciucchi B, Holz J. *In vitro* cytotoxicity and dentin permeability of HEMA. J Endod. 1996;22:244-8.

4- Hanks CT, Wataha JC, Parsell RR, Strawn SE, Fat JC. Permeability of biological and synthetic molecules through dentine. J Oral Rehabil. 1994;21:475-87.

5- Kitamura C, Kimura K, Nakayama T, Toyoshima K, Terashita M. Primary and secondary induction of apoptosis in odontoblasts after cavity preparation of rat molars. J Dent Res. 2001;80:1530-4.

6- Kitamura C, Nishihara T, Ueno Y, Chen K-K, Morotomi T, Yano J, et al. Effects of sequential exposure to lipopolysaccharide and heat stress on dental pulp cells. J Cell Biochem. 2006;99:797-806.

7- Kitamura C, Ogawa Y, Morotomi T, Terashita M. Differential induction of apoptosis by capping agents during pulp wound healing. J Endod. 2003;29:41-3.

8- Lu Y, Liu T, Li H, Pi G. Histological evaluation of direct pulp capping with a self-etching adhesive and calcium hydroxide on human pulp tissue. Int Endod J. 2008;41:643-50.

9- Mantellini MG, Botero TM, Yaman P, Dennison JB, Hanks CT, Nör JE. Adhesive resin induces apoptosis and cell-cycle arrest of pulp cells. J Dent Res. 2003;82(8):592-6.

10- Murray PE, Smyth TW, About I, Remusat R, Franquin JC, Smith AJ. The effect of etching on bacterial microleakage of an adhesive composite restoration. J Dent. 2002;30:29-36.

11- Rikitake Y. Immortalization of human dental pulp cells with transfecting of the plasmid, pMT1-neo. Kokubyo Gakkai Zasshi. 1989;56:540-61.

12- Schweikl H, Spagnuolo G, Schmalz G. Genetic and cellular toxicology of dental resin monomers. J Dent Res. 2006;85:870-7.

13- Ueno Y, Kitamura C, Terashita M, Nishihara T. Re-oxygenation improves hypoxia-induced pulp cell arrest. J Dent Res. 2006;85:824-8.

Promoting effects of thymosin β4 on granulation tissue and new bone formation after tooth extraction in rats

Kou Matsuo, DDS, PhD,[a] Yosuke Akasaki, DDS,[b] Kazutaka Adachi, DDS,[b]
Min Zhang, MD, PhD,[c] Ayataka Ishikawa, DDS, PhD,[c] Eijiro Jimi, DDS, PhD,[d]
Tatsuji Nishihara, DDS, PhD,[e] and Ryuji Hosokawa, DDS, PhD,[f] Kitakyushu, Japan
KYUSHU DENTAL COLLEGE

Objectives. The aim of this study was to evaluate the effects of thymosin β4 (TB4) on wound healing after tooth extraction in rats.
Study design. After extraction of the rats' mandibular first molar teeth, a synthetic partial peptide of TB4 was injected intraperitoneally at the time of extraction and every day thereafter for 6 days. Control subjects for the treatment received identical amounts of phosphate-buffered saline solution in the same manner. Histologic analysis, apoptosis assay, and reverse-transcription polymerase chain reaction were performed.
Results. The overall data showed that TB4 treatment suppressed apoptosis and inflammation; it accelerated the process of wound healing, including new bone formation.
Conclusions. The findings demonstrated not only the usefulness of the TB4 partial peptide in wound healing of tooth extraction sockets, but also its potential application for bone regeneration and osteogenesis in bone and bone-related tissues. **(Oral Surg Oral Med Oral Pathol Oral Radiol Endod 2011;xx:xxx)**

Thymosin was originally isolated from calf thymus and was considered to be a thymic hormone consisting of a single polypeptide,[1-3] but it is now known to consist of a mixture of small polypeptides.[4-6] Thymosins are now divided into 3 main groups, i.e., α-, β-, and γ-thymosins, according to their isoelectric points. The β-thymosins (TBs), whose isoelectric points range from 5.0 to 7.0, are a family of highly conserved polar 5-kDa polypeptides consisting of 40-44 amino acids (AA).[5,6] To date, 15 TB have been isolated from various vertebrates and invertebrates. Thymosin β4 (TB4) is the most abundant type of TB in most mammalian tissues, representing ~70%-80% of the total TB content. The complete TB4 amino acid sequence of 43 residues is invariant among most known mammalian sources, such as human, rat, mouse, cat, calf, horse, pig, sheep, and chicken, with the exception of rabbit.[5] Thymosins β10 (TB10) and β15 (TB15) are also present in human, rat, and mouse tissues.

TBs are often referred to as "G-actin–sequestering peptides," meaning that TBs bind monomeric globular actin (G-actin) in a 1:1 complex and prevent polymerization into actin filaments.[5-8] Besides being simple actin monomer–buffering proteins, recent studies, especially regarding TB4, have revealed that TBs are multifunctional polypeptides involved in angiogenesis,[9-11] wound healing,[12-18] antiapoptotic activity,[18-20] and antiinflammatory reactions.[13,21] Nonetheless, there have been very few reports of TBs relating directly to the fields of dental research or clinical dentistry.[22-24]

Based on the background described above, we initiated a basic experiment to investigate the functional analysis of TB4 in wound healing after tooth extraction, with the ultimate aim of clinical dental application, including regenerative therapy. This report shows a new functional aspect of TB4, including its possible role in bone regeneration and osteogenesis.

MATERIAL AND METHODS

All protocols for the present experiment were reviewed and approved by the Council on Animal Care at Kyushu Dental College (approval number 07-051).

Synthetic peptide

A 20-AA partial peptide was synthesized (Sigma Genosys, Hokkaido, Japan), corresponding to AAs 17-36 in the full-length (AAs 1-43) TB4 polypeptide[5,6] (Fig. 1).

Supported by a grant-in-aid for Scientific Research (C) 20592179 from the Japan Society for the Promotion of Science (to K.M.), a grant-in-aid from Kyushu Dental College Internal Grants (to K.M.), and a grant-in-aid from Kyushu Dental College Alumni Association Grants (to K.M.).
[a]Associate Professor, Department of Biosciences.
[b]Resident, Department of Oral Functional Reconstruction.
[c]Assitant Professor, Department of Biosciences.
[d]Professor, Department of Biosciences.
[e]Professor, Department of Health Promotion.
[f]Professor, Department of Oral Functional Reconstruction.
Received for publication Apr. 27 2011; accepted for publication May 28, 2011.
1079-2104/$ - see front matter

doi:10.1016/j.tripleo.2011.05.025

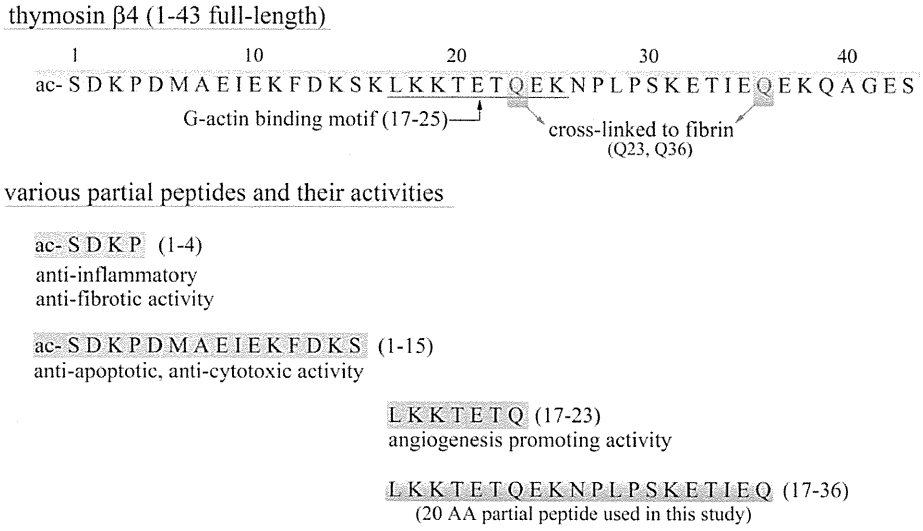

Fig. 1. Amino acid sequences and activities of thymosin β4 and its partial peptides.

Table I. PCR primer sets used in this study

*Gene (accession number)**	*Forward primer sequences (5′-3′)*	*Reverse primer sequences (5′-3′)*	*Size (bp)*
G3PDH (M17701)	TGAAGGTCGGTGTCAACGGATTTGGC	CATGTAGGCCATGAGGTCCACCAC	983
VEGF-A (NM_031836)	GCCCATGAAGTGGTGAAGTT	ACTCCAGGGCTTCATCATTG	172
VEGF-B (NM_053549)	AGGGAGGTGGTGGTACCTCTGAGCA	TGGTCTGCATTCACATTGGCTGTGT	231
VEGF-C (NM_053653)	GATGTGGGGAAGGAGTTTGGAGCAG	ATTGTGACTGGTTTGGGGCCTTGAG	188
VEGF-D (AF014827)	TTGGGGCTTCAAACTTTGCTTCTGG	ACTGAAGCCCTGCACCAGGTACACA	173
Angpt1 (NM_053546)	AAGGCGAGTGCTGGCAGTACAATGA	CCCTTTGCAGAGCGTTGGTGTTGTA	229
Angpt2 (NM_134454)	TGCAGATAAATCCCGGGACCACATT	TGTCAAGCACAAGACGGAACAACGA	168
VEGFR-1 (NM_019306)	CATCGGCCATCATCTGAATGTGGTT	GCTGACACTGTCTAGGCGGGGTTTC	232
VEGFR-2 (U93306)	ATTGAGGCAGATGCCTTTGGAATCG	ACCCAGCAGGTTCACCACATTGAGA	165
VEGFR-3 (NM_053652)	GTCATTGACACCGGGGACAGCCTAT	GCCCTCAATCCGGGCCTTGATATAC	249
Tie2 (NM_001105737)	CAGGGCAAAAATGAAGACCAGCACA	CCTCCAAGGTCTTTAGGGGCTGGAA	191
MMP2 (NM_031054)	GGAGAAGGCTGTGTTCTTCG	CGGGTCCATTTTCTTCTTCA	214
ILK (NM_133409)	AATGTCCCCGGCTCAGGATTTTCTC	TTGGCTCTGGTCCACAACGAAATTG	167
HGF (NM_017017)	GCATGATGTGGGGGACCAAACTTCT	GCCCTTGTTTCTGATGCACCTGTTG	242
TGF-β1 (NM_021578)	AAAGAAGTCACCCGCGTGCTAATGG	CCAAGGTAACGCCAGGAATTGTTGC	233
IL-1α (NM_017019)	ATCCGCAGCTTTCCCAGAGCTGTTA	ATGCCATGCGAGTGACTTAGGACGA	200
IL-1β (NM_031512)	GGGATCCTCTCCAGTCAGGCTTCCT	TGCTCTCATCTGGACAGCCCAAGTC	186
IL-6 (NM_012589)	GCCCACCAGGAACGAAAGTCAACTC	TGGTCTGTTGTGGGTGGTATCCTCTG	179
TNF-α (NM_012675)	TCCTTCCTTCCTTCCCTCCCTCAGA	GTTGGCCTGAAGACAGCTTCCCAAC	209
BMP-2 (NM_017178)	TTTTGGCCACGACGGTAAAGGACAT	AGTTCAGGTGATCAGCCAGGGGAAA	218
BMP-4 (NM_012827)	GGGGAGGAGGAGGAAGAAGAGCAGA	CACCTCATTCTCTGGGATGCTGCTG	186
BMP-7 (XM_001053727)	CCAGAACCGCTCCAAGACTCCAAAG	AGGGAAGGCACACTCTCCCTCACAG	199
Osterix (AY177399)	CCCAGCATGTCCTACCCCAAGATGT	CCAGCCGCTCTAGCTCCTGACAGTT	186
ALP (NM_013059)	GACAAGAAGCCCTTCACAGCCATCC	GCCATGACGTGGGGGATGTAGTTCT	239
Osteocalcin (NM_013414)	AGCAGGAGGGCAGTAAGGTGGTGAA	ATGCCCTAAACGGTGGTGCCATAGA	196

*Accession number of GenBank. The primer sequences were designed based on rat mRNA sequences obtained from GenBank. *G3PDH*, glyceraldehyde-3-phosphate dehydrogenase; *VEGF*, vascular endothelial growth factorAngpt angiopoietin; *VEGFR*, vascular endothelial growth factor receptor; *Tie*, tyrosine kinase with Ig-like loops and epidermal growth factor homology domains; *MMP*, matrix metalloproteinase; *ILK*, integrin-linked kinase; *HGF*, hepatocyte growth factor; *TGF*, transforming growth factor; *IL*, interleukin; *TNF*, tumor necrosis factor; *BMP*, bone morphogenetic protein; *ALP*, alkaline phosphatase; *bp*, base pair.

Animals

Ninety-six 6-week-old male Wistar rats (Charles River Laboratories, Yokohama, Japan) were used. After tooth extraction, they were given a powdered diet and water ad libitum.

Tooth extraction and administration of thymosin β4

Under pentobarbital anesthesia, mandibular first molars were extracted using custom-made dental forceps (Seiwa Riken, Tokyo, Japan). The rats received an

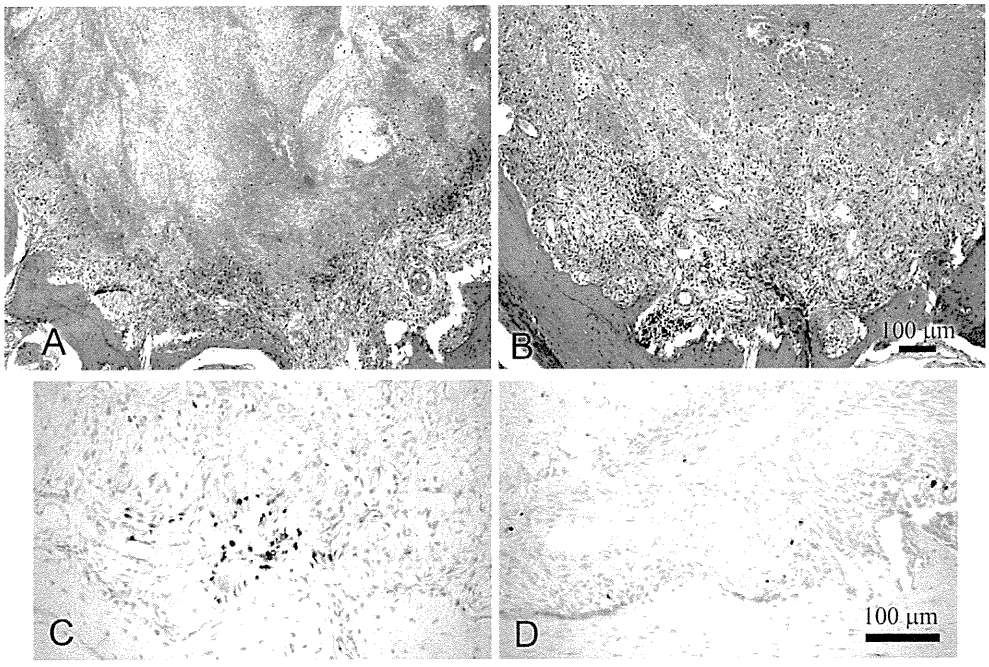

Fig. 2. Representative hematoxylin-eosin (**A** and **B**) and terminal deoxynucleotide transferase–mediated dUTP nick-end labeling (TUNEL) (**C** and **D**) stained sections of tooth sockets on day 1 from the control (**A** and **C**) and TB4-treated (**B** and **D**) groups. On day 1, the control group socket is filled mostly with a blood clot (**A**). A slightly greater amount of granulation tissue is noted in the bottom of the socket in the TB4-treated group (**B**). A lower number of TUNEL-positive apoptotic cells are observed in the TB4-treated group (**D**) than in the control group (**C**). The TUNEL specimens were counterstained with methyl green.

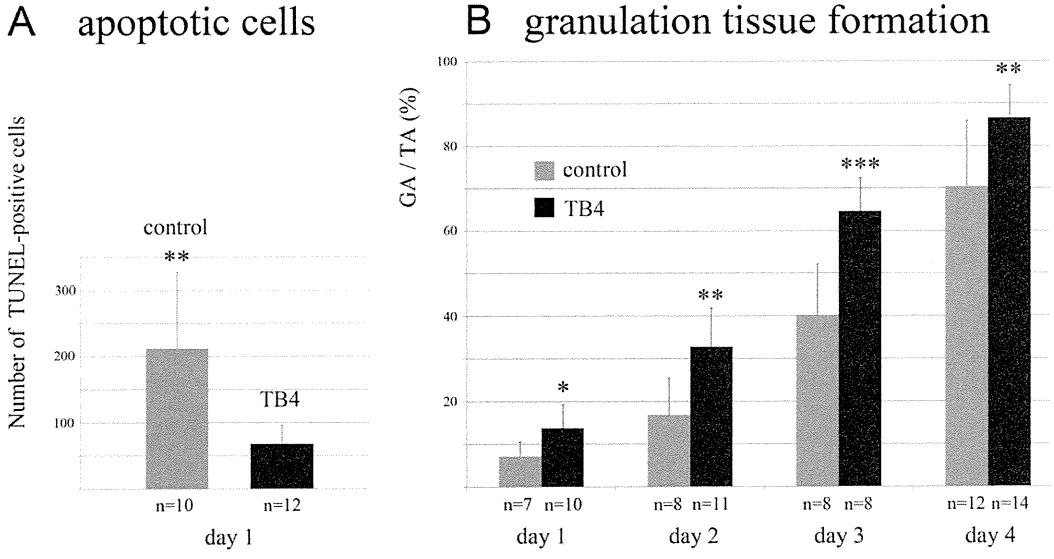

Fig. 3. Number of apoptotic cells (**A**) and percentage of granulation tissue area (GA) relative to the tooth extraction socket area (TA) (**B**). Data are expressed as mean and SD. Significant differences between control and TB4-treated groups are indicated by asterisks (*$P < .05$; **$P < .01$; ***$P < .001$).

intraperitoneal injection of TB4 synthetic peptide solution (50-μg peptide in 300 μL phosphate-buffered saline solution [PBS], pH 7.4) immediately after tooth extraction and every day thereafter for 6 days. Control subjects received an equivalent amount of PBS intraperitoneally under the same schedule.

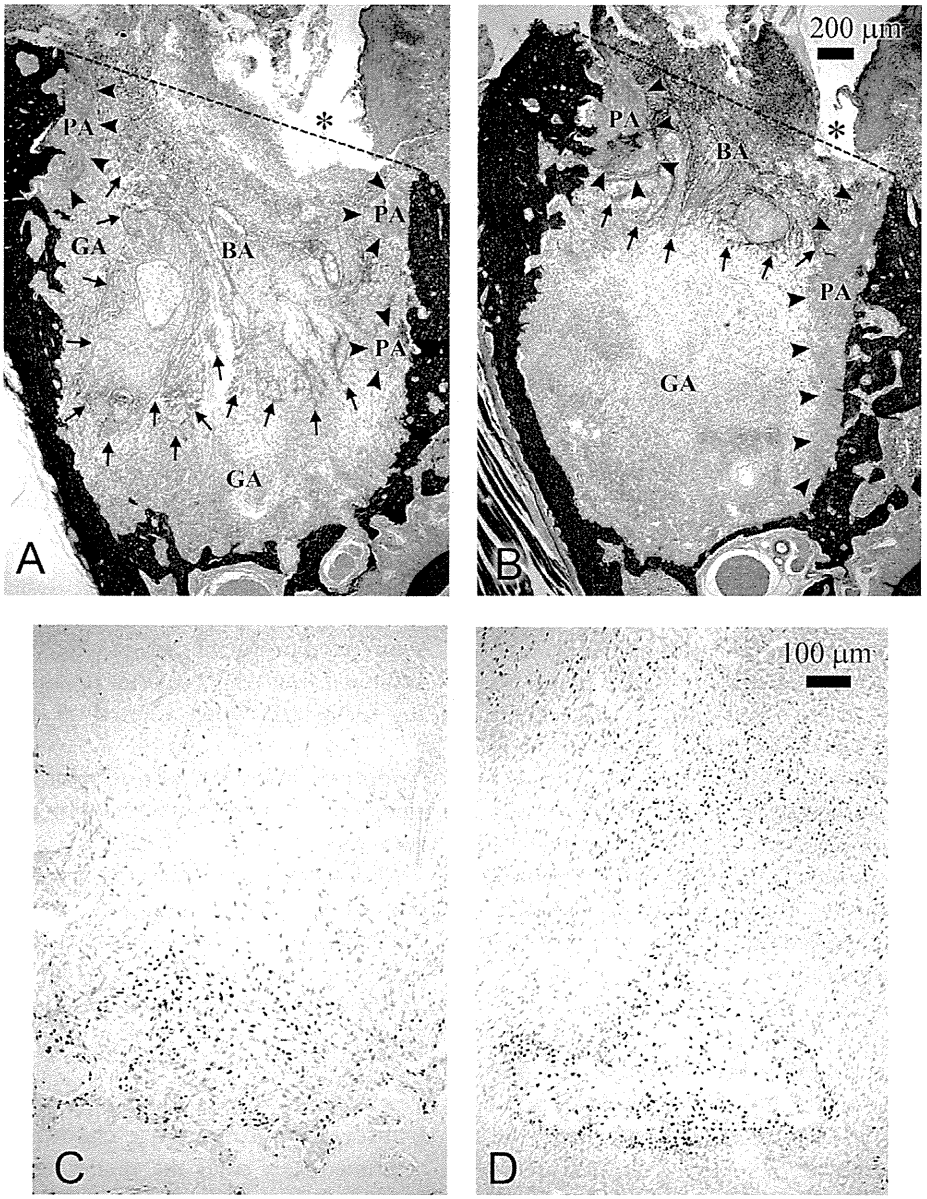

Fig. 4. Representative phosphotungstic acid hematoxylin (PTAH) staining (**A** and **B**) and immunostaining for osterix (**C** and **D**) on day 3 from control (**A** and **C**) and TB4-treated (**B** and **D**) groups. *GA*, granulation tissue area; *BA*, blood clot area; *PA*, periodontal ligament area. The *dashed line* (*) denotes the upper limit of the tooth extraction socket area (TA). *Arrows* indicate the border between GA and BA. Arrowheads indicate the border between PA and GA or PA and BA. Accelerated formation of granulation tissue on day 3 in the TB4-treated group is seen (**B**) compared with the control group (**A**). Osterix-positive cells are mainly observed on day 3 at the bottom of the socket (**C**). More osterix-positive cells have spread into the center of the GA from the bottom of the socket in the TB4-treated group (**D**). The immunostained sections were counterstained with methyl green.

Histologic and immunohistochemical analyses

Treated rats were killed under pentobarbital anesthesia on days 1, 2, 3, 4, and 6 after tooth extraction. The mandibles were removed, fixed in 10% neutral-buffered formalin overnight, and then decalcified in 10% EDTA containing 7% sucrose for up to 21 days. The completely decalcified mandibles were sectioned vertically in the buccolingual direction to obtain the maximum exposed surface of the socket corresponding to the distal root of the extracted tooth. The samples were then paraffin embedded and sectioned at a thickness of 5 μm. These serial sections were stained with hematoxylin-eosin (H-E) and phosphotungstic acid hematoxylin (PTAH). Immunohisto-

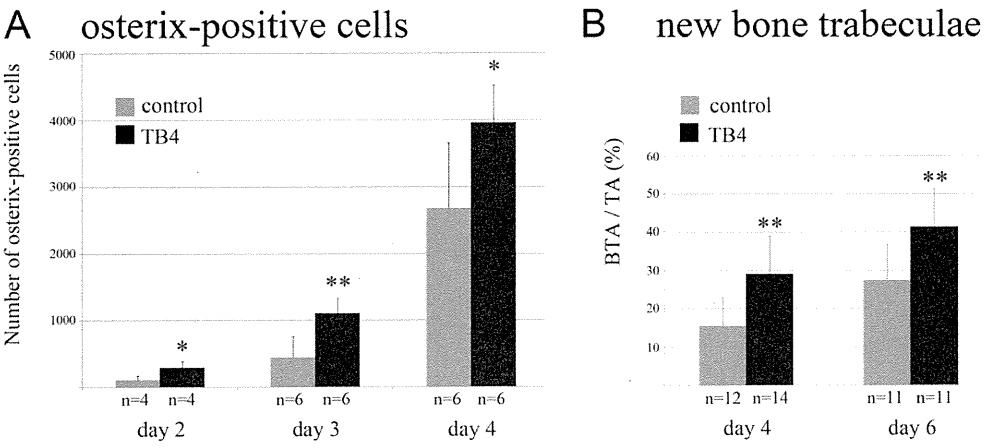

Fig. 5. Number of osterix-positive cells (**A**) and percentage of newly formed bone trabeculae area (TBA) relative to the tooth extraction socket area (TA) (**B**). Data are expressed as mean and SD. Significant differences between control and TB4-treated groups are indicated by asterisks (*$P < .05$; **$P < .01$).

chemical staining was performed using anti-Sp7/osterix rabbit polyclonal antibody (ab22552, 1:200; Abcam, Cambridge, U.K.) and antiperiostin rabbit polyclonal antibody (ab14041, 1:150; Abcam) as the first antibodies. Histofine Simple Stain Rat Max-PO (Multi) (Nichirei Biosciences, Tokyo, Japan) was used as the second antibody. Detection was performed with the Immpact DAB peroxidase substrate kit (Vector Laboratories, Burlingame, CA). Nuclear counterstaining was carried out with the use of either methyl green or hematoxylin.

The digital images of the histologic sections were analyzed by Adobe Photoshop CS4 Extended (Adobe Systems, San Jose, CA) and ImageJ, version 1.44a (National Institutes of Health, Bethesda, MD) software. To simplify the calculation of the area, the tooth extraction socket area (TA) was defined as the area bounded by a curve along the medial border of the alveolar bone and a straight line (upper limit of TA) connecting the 2 ends of the curve. The granulation tissue area (GA) was distinguished from the blood clot area (BA) and periodontal ligament area (PA). BA was defined as the area stained deep blue by PTAH. PA was confirmed by immunohistochemical staining for periostin on the serial sections. The percentage of GA relative to TA was calculated for each PTAH-stained section. When we assessed granulation tissue formation, we did not exclude areas of newly formed bone trabeculae or osteoid tissue from GA. For the assessment of new bone and osteoid formation in the tooth extraction socket, the percentage of newly formed bone trabecular area (BTA) relative to TA was calculated from the digital images of the H-E sections. The BTA, including osteoid, was confirmed by immunostaining for osterix on serial sections. For further assessment of new bone and osteoid formation, all cells positively immunostaining for osterix were counted on the digital images.

Apoptosis assay based on terminal deoxynucleotide transferase–mediated dUTP nick-end labeling method

Serial unstained sections from the paraffin-embedded tissues were used for apoptosis assay with the ApoMark Apoptosis Detection Kit (Exalpha Biologicals, Maynard, MA) according to the manufacturer's protocol. Apoptotic cells were counted on the digital images.

Preparation of total RNA and reverse-transcription polymerase chain reaction

Immediately after the rats were killed, at either 9 hours or 3 days after tooth extraction, granulation tissue was isolated from the socket with a 27-gauge needle, and then total RNAs were prepared from this with the use of the SV total RNA isolation system (Promega, Madison, WI).

Reverse-transcription polymerase chain reaction (RT-PCR) was performed using the Titanium One-Step RT-PCR kit (Clontech, Mountain View, CA) according to the manufacturer's instructions. The primers used in our study are summarized in Table I. The RT-PCR products after 25-35 PCR cycles were electrophoresed on 1%-2% agarose gel, visualized with ethidium bromide staining under ultraviolet light exposure, photographed using a digital camera (PowerShot A640; Canon, Tokyo, Japan), and stored as digital images. The integrated density (IntDen) of each band was calculated with the use of ImageJ. The relative mRNA levels of target genes were expressed as a percentage of

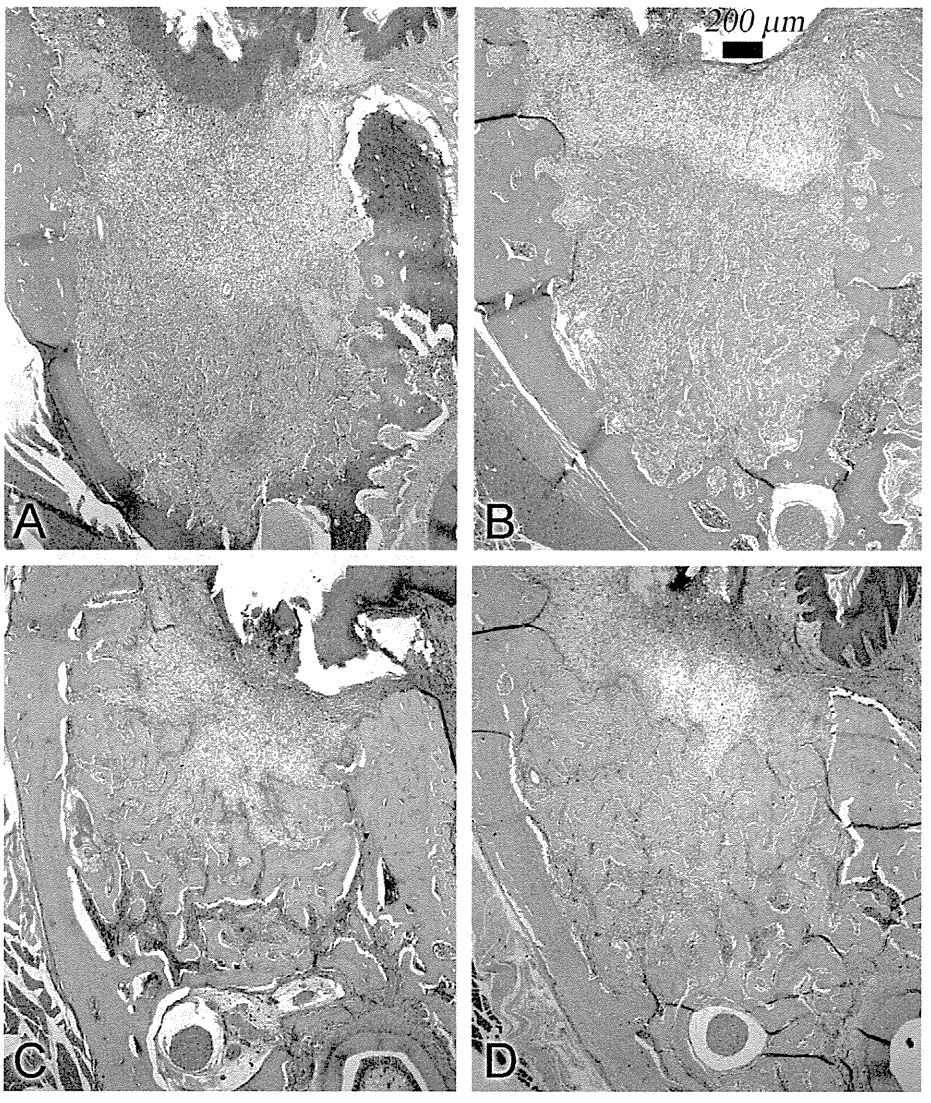

Fig. 6. Representative hematoxylin-eosin sections from days 4 (**A** and **B**) and 6 (**C** and **D**) in the control (**A** and **C**) and TB4-treated (**B** and **D**) groups. A greater amount of newly formed bone trabeculae is noted in the TB4-treated group on day 4 (B) than in the control group (**A**). On day 6, the socket in the TB4-treated group (**D**) still shows a greater amount of bone trabeculae than in the control group (**C**).

the ratio of target gene IntDen relative to glyceraldehyde-3-phosphate dehydrogenase IntDen. Analysis was performed 4 times using different batches of total RNA samples. The results are shown as mean values with standard deviations (n = 4).

Data analysis

The statistical significance of differences in the mean values between the 2 groups was assessed by Student *t* test if variances were equal as determined by an *F* test, otherwise by Welch *t* test. All tests were 2 tailed, with differences reported as significant when $P < .05$.

RESULTS

Comparative histologic findings in the healing process after tooth extraction

The extraction sockets on day 1 in the control group were filled mostly with blood clots, although remaining periodontal tissue and only a very small amount of granulation tissue were observed at the bottom. In contrast, there was a slightly greater amount of granulation tissue in the bottom of sockets in the TB4-treated group. In addition, the TB4-treated group had fewer apoptotic cells than the control group (Figs. 2 and 3). On day 2, the sockets in the control group still contained only a small amount of granulation tissue at the